GEOLOGICAL SURVEY OF CANADA
OPEN FILE 7856

Targeted Geoscience Initiative 4: Canadian Nickel-Copper-Platinum Group Elements-Chromium Ore Systems — Fertility, Pathfinders, New and Revised Models

Geochemistry and petrogenesis of the Black Thor intrusive complex and associated chromite mineralization, McFaulds Lake greenstone belt, Ontario

Heather J.E. Carson[1], C. Michael Lesher[1], and Michel G. Houlé[2]

[1]Laurentian University, Sudbury, Ontario
[2]Geological Survey of Canada, Québec, Quebec

2015

This publication is available for free download through GEOSCAN (http://geoscan.nrcan.gc.ca/)

Recommended citation

Carson, H.J.E., Lesher, C.M., and Houlé, M.G., 2015. Geochemistry and petrogenesis of the Black Thor intrusive complex and associated chromite mineralization, McFaulds Lake greenstone belt, Ontario, *In:* Targeted Geoscience Initiative 4: Canadian Nickel-Copper-Platinum Group Elements-Chromium Ore Systems — Fertility, Pathfinders, New and Revised Models, (ed.) D.E. Ames and M.G. Houlé; Geological Survey of Canada, Open File 7856, p. 87–102.

Publications in this series have not been edited; they are released as submitted by the author.

Contribution to the Geological Survey of Canada's Targeted Geoscience Initiative 4 (TGI-4) Program (2010–2015)

TABLE OF CONTENTS

Geochemistry and petrogenesis of the Black Thor intrusive complex and associated chromite mineralization, McFaulds Lake greenstone belt, Ontario

Heather J.E. Carson[1*], C. Michael Lesher[1], and Michel G. Houlé[2]

[1]Mineral Exploration Research Centre, Department of Earth Sciences, Goodman School of Mines, Laurentian University, 935 Ramsey Lake Road, Sudbury, Ontario P3E 2C6
[2]Geological Survey of Canada, 490 rue de la Couronne, Québec, Quebec G1K 9A9
*Corresponding author's e-mail: hcarson@laurentian.ca

ABSTRACT

The Black Thor intrusive complex (BTIC) contains a conduit-hosted, stratiform Cr-Ni-Cu-(PGE) deposit with a very large amount of chromite for an intrusion of its size. Most conduit-hosted stratiform deposits are Archean, formed from komatiitic magmas containing approximately 3000 ppm Cr_2O_3, and are typically saturated in chromite. The fundamental problem in understanding the genesis of the BTIC deposit and other deposits of this type is explaining how such large quantities of chromite crystalized from a magma that normally crystallizes only small amounts chromite and normally have a chromite:olivine abundance ratio of ~1:60. Current genetic models, such as in situ crystallization (by oxidation, pressure increase, magma mixing, and/or wholesale assimilation of felsic rocks or iron formation) or physical transportation of chromite slurries do not provide a wholly satisfactory explanation for the high abundance of chromite in this type of deposit. We are testing an alternative model: partial assimilation (as opposed to wholesale assimilation) of local oxide-silicate-facies iron formation by a Cr-rich magma. As low-Mg komatiite is saturated in chromite, the magma may dissolve the silicate component (quartz/chert and Fe-silicate minerals) of the iron formation, but would be unable to dissolve the oxide component (magnetite). Through interaction with the high-temperature (1400°C) Cr-rich magma, the fine-grained magnetite could be upgraded via diffusion to chromite during transportation within the conduit. This upgrading is similar to the upgrading of barren sulphide xenomelts that has been proposed for Ni-Cu-(PGE) deposits.

INTRODUCTION

The Black Thor intrusive complex (BTIC) is part of the Neoarchean "Ring of Fire" Intrusive Suite (RoFIS) located within the 2.7–2.8 Ga McFaulds Lake greenstone belt (MLGB) in the James Bay Lowlands of northern Ontario. The Black Thor chromite deposit, discovered in 2006, is one of the largest and best-preserved chromite deposits in the world. It contains ~102 Mt of chromite-mineralized material in a zone measuring up to 3 km in strike length and likely extends ~15 km to the Big Daddy, Black Creek, Black Horse, and Blackbird deposits. The bulk ore of the Black Thor deposit has an aggregate thickness of up to 100 m and an average grade of 31% Cr_2O_3 (Weston and Shinkle, 2013).

Previous work in the area includes a M.Sc. thesis on the nearby Blackbird chromite deposit (Azar, 2010), a paper on the Eagle's Nest Ni-Cu-(PGE) deposit (Mungall et al., 2010), and a Ph.D. thesis on the chemistry of chromite from the Black Thor, Black Label, and Big Daddy chromite deposits in the MLGB Black Thor chromitite layers (Laarman, 2014). However, the BTIC as a whole has not been studied in detail and is characterized only by airborne and ground geophysics and exploration-scale core logs (Tuchscherer et al., 2010). The main objective of this research is to establish the stratigraphy, geochemistry, and petrogenesis of the BTIC and associated chromium and nickel-copper-platinum group element (PGE) mineralization.

METHODOLOGY

Core logging and sampling were completed in May-June 2012 and June-July 2013 (Fig. 1). One hundred and twenty-three finely ground slabs from drillhole BT-11-196 were studied using a binocular microscope; 178 polished thin sections were studied in transmitted and reflected light using a compound petrographic microscope. Three hundred and twenty-four whole-rock samples were analyzed for major, minor, and trace elements by a combination of wavelength-dispersive X-ray fluorescence spectrometry, inductively coupled plasma (ICP) atomic emission spectrometry, and ICP

Carson, H.J.E., Lesher, C.M., and Houlé, M.G., 2015. Geochemistry and petrogenesis of the Black Thor intrusive complex and associated chromite mineralization, McFaulds Lake greenstone belt, Ontario *In:* Targeted Geoscience Initiative 4: Canadian Nickel-Copper-Platinum Group Elements-Chromium Ore Systems — Fertility, Pathfinders, New and Revised Models, (ed.) D.E. Ames and M.G. Houlé; Geological Survey of Canada, Open File 7856, p. 87–102.

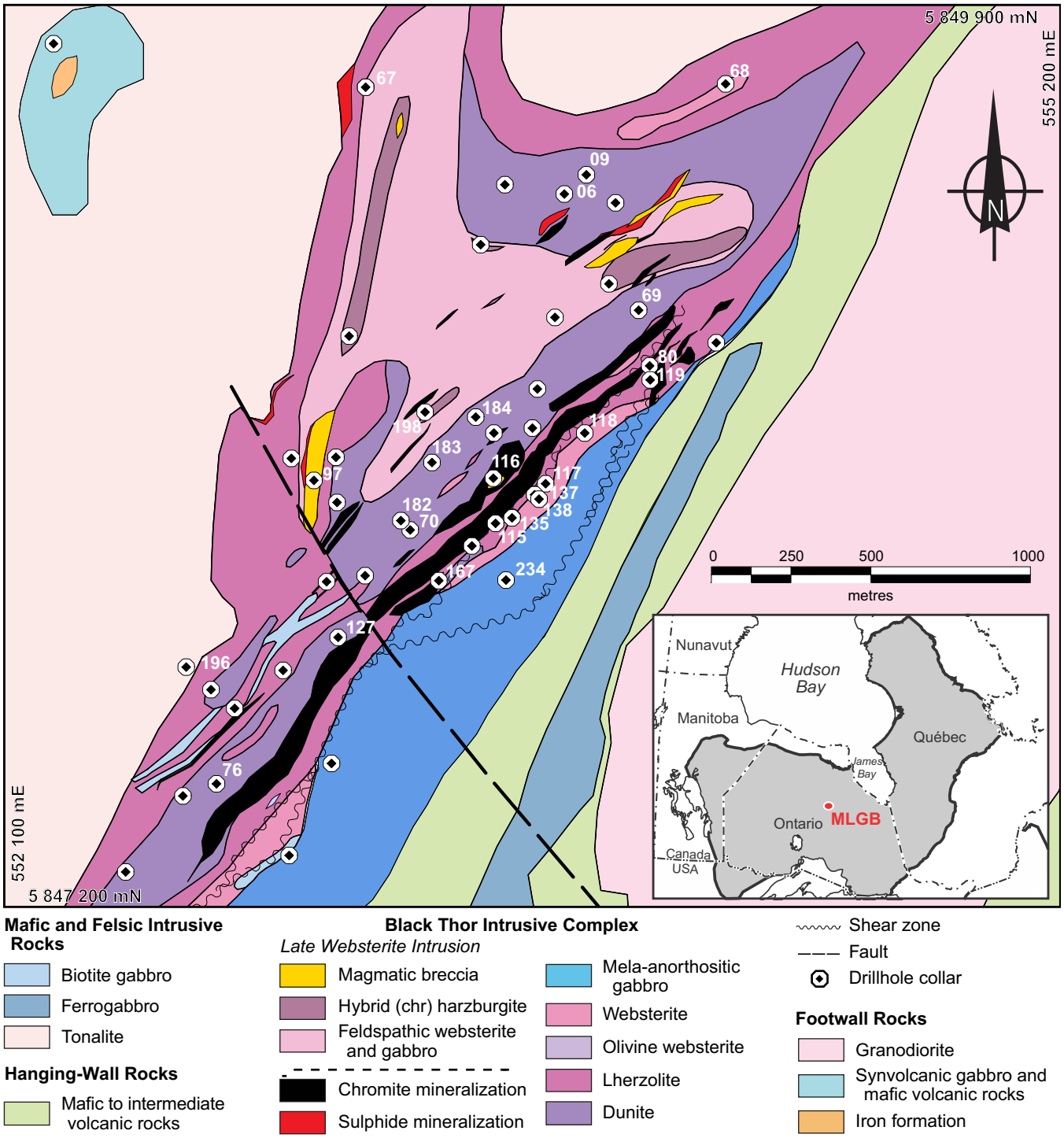

Figure 1. Geological map of the Black Thor intrusive complex showing the locations of diamond drillholes (DDH) that were logged and sampled in the course of this study (modified from Weston and Shinkle, 2013). Diamond drillhole identifications are given for those mentioned in the text. The first parts of the DDH identifications have been omitted for simplicity, DDH identifications: BT-08-06, 09; BT-09-67, 68, 69, 70, 76, 80; BT-10-115, 116, 117, 118, 119, 127, 135, 137, 138, 167; BT-11-182, 183, 184, 198, 196; and BT-12-234. MLGB: McFaulds Lake greenstone belt.

mass spectrometry. Chromite and associated melt inclusions and silicate minerals from 13 samples have been analyzed thus far by a combination of energy-dispersive X-ray emission spectrometry (XRES) using a scanning electron microscope, wavelength-dispersive XRES using an electron probe microanalyzer, and laser-ablation ICP-MS. Three-dimensional X-ray tomographic studies, O, S, Cr-Ni-Fe, Nd, Hf, and Os isotope analyses, and computer models of the miner-

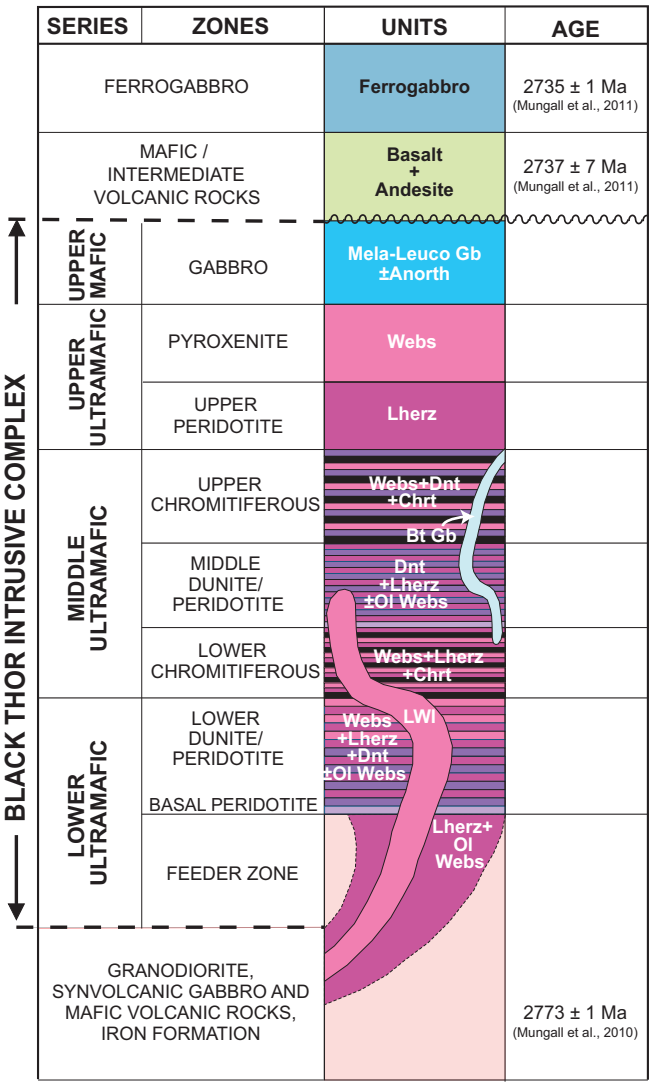

Figure 2. Schematic cross-section through the Black Thor intrusive complex (modified from Carson et al., 2013). Abbreviations: Anorth = anorthosite, Bt Gb = biotite gabbro, Chrt = chromitite, Dnt = dunite, Lherz = lherzolite, LWI = late websterite intrusion, Mela-Leuco Gb = mela- to leucogabbro, Ol Webs = olivine websterite, Webs = websterite.

alogical and geochemical data will be done later in 2015.

RESULTS

Geology of the Black Thor Intrusive Complex

The BTIC is a semi-conformable, funnel-shaped intrusion that has been structurally rotated into a subvertical orientation (Fig. 1). It is subdivided into four series (from stratigraphic base to top; Fig. 2): 1) a lower ultramafic series of interlayered dunite and lherzolite and minor olivine websterite (Fig. 3a–e); 2) a middle ultramafic series of interlayered dunite, lherzolite, and websterite with a thin lower chromitite zone (Black Label horizon; Fig. 4a–d) and a thick upper chromitite zone (Black Thor horizon; Fig. 4e–l); 3) an upper ultramafic

Table 1. Primary and hydrated mineralogy of the main rock type of the Black Thor intrusive complex.

Lithology	Igneous Mineralogy	Hydrated Mineralogy
Dunite	Ol-(Chr)	Atg/Lz-Mag-(Chl)-(Iow)-Tc
Lherzolite	Ol-Opx-(Chr)	Atg/Lz-Mag-Tr-Chl-Act-Tc
Chromitite	Chr-Ol	Atg/Lz-Mag-(Chl) -(Käm)-Tc
Ol Websterite	Opx-Ol-Chr	Act-MgHb-Käm±NiClc-Chl
Websterite	Opx-Cpx	Act-Chl-Tc
Melagabbro	Cpx-Plag	Act-Chl-(Czo)
Mesogabbro	Plag-Cpx	Ab-Chl-Czo-Act
Leucogabbro	Plag-Cpx-Ilm	Ab-Chl-Czo-Act-Ms-Ttn

Abbreviations: Ab = albite; Act = actinolite; Atg/Lz = antigorite/lizardite; Chl = chlorite; Chr = chromite; Cpx = clinopyroxene; Czo = clinozoisite; Ilm = ilmenite; Iow = iowite; Käm = kämmererite; Mag = magnetite; MgHb = magnesiohornblende; Ms = Muscovite; NiClc = Ni-clinochlore; Ol = olivine; Opx = orthopyroxene; Plag = plagioclase; Tc = Talc; Tr = tremolite; Ttn = titanite.

series composed of lherzolite, websterite, feldspathic websterite, and olivine websterite (Fig. 3f–h); and 4) a mafic series consisting of mela-, meso-, and leucogabbro with lesser anorthosite (Fig. 3i–l). It was originally not clear whether the upper mafic series was part of the BTIC, but gradational contacts with the underlying ultramafic rocks indicate that it is part of the intrusion. In places these rocks interfinger with (and are interpreted to intrude) overlying mafic volcanic rocks of the MLGB.

After accumulation and partial solidification of the BTIC, a late websterite intrusion (LWI) was emplaced into the lower and middle ultramafic series rocks and locally brecciated the Black Label chromitite horizon. The BTIC was later metamorphosed to lower-greenschist facies, but most of the rocks contain well preserved igneous textures, and relict igneous chromite, pyroxene, and olivine are variably preserved (Table 1). The term "meta" will be omitted for simplicity in this contribution.

Cr and Ni-Cu-(PGE) Mineralization

Chromite mineralization displays a range of textures that are distinguished based on chromite content: massive (>90%), semi-massive (90–75%), matrix (75–50%), net-textured (50–30%), heavily disseminated (30–10%), and lightly disseminated (<10%). Chromite is uniformly fine grained (0.1–0.2 mm) and forms networks between coarse-grained (<2 cm) altered pyroxene oikocrysts and between fine-grained (~5 mm) serpentinized olivine grains (Fig. 4). The Black Thor chromitite horizon (this study) and the undisrupted parts of the Black Label chromitite horizon (Mehrmanesh et al., 2013) contain thinly laminated to thickly bedded massive chromitite layers that alternate with partially continuous layers of serpentinized dunite. Brecciated parts of Black Label (Spath et al., 2015) contain angular to amoeboid clasts of chromitite,

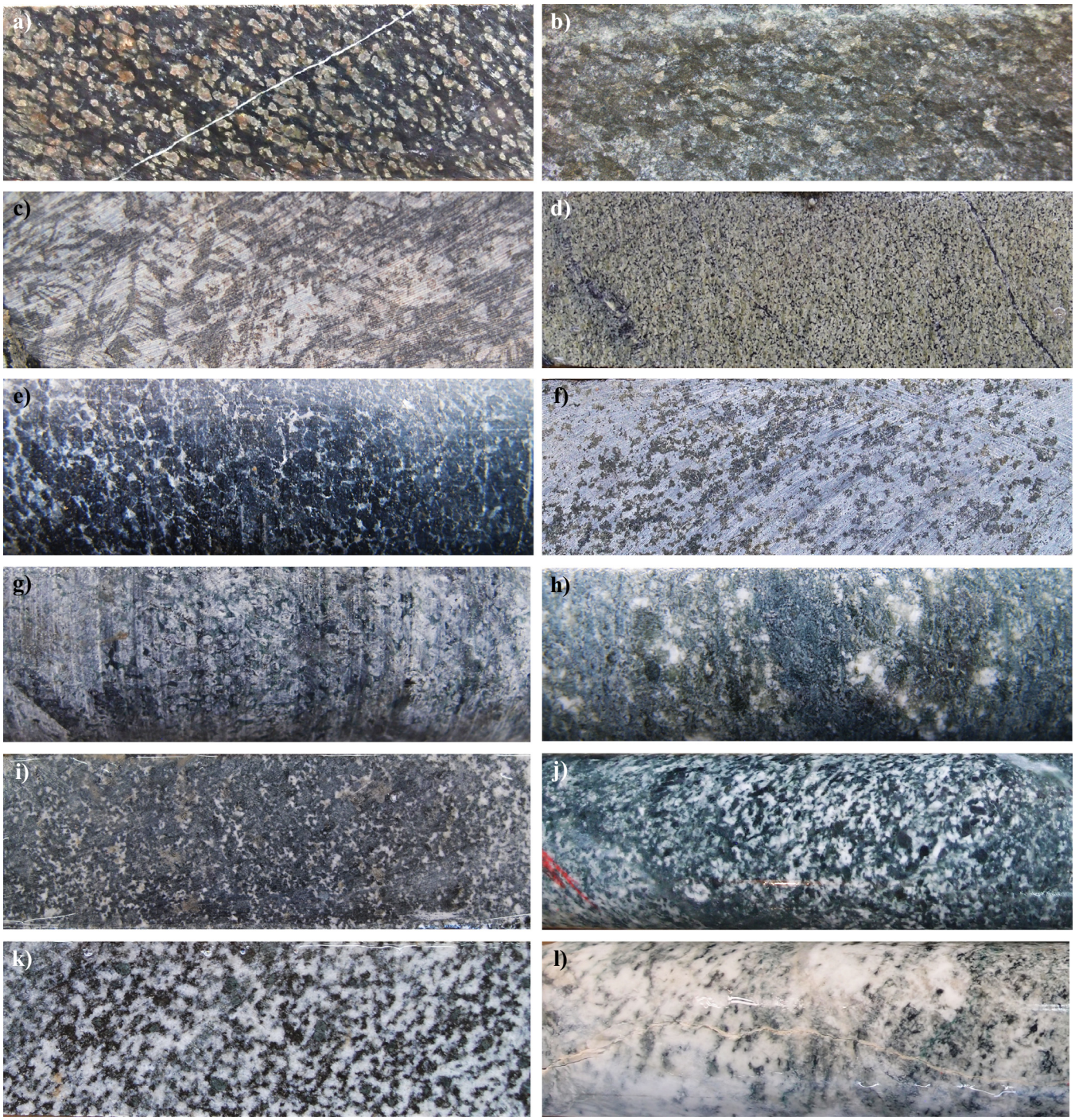

Figure 3. Photographs of drill cores showing typical rock types of the lower ultramafic series (a to e), the upper ultramafic series (f to h), and the mafic series (i to l) of the Black Thor intrusive complex. **a)** Basal peridotite (harzburgite); BT-09-70/37.70 m. **b)** Late pyroxenite; BT-11-198/42.00 m. **c)** Olivine spinifex-textured olivine, BT-09-97/136.09 m. **d)** Heavily serpentinized dunite; BT-09-70/98.11 m. **e)** Serpentinized peridotite, BT-11-196/180.10 m. **f)** Olivine pyroxenite; BT-10-115/83.85 m. **g)** Pyroxenite; BT-12-234/38.05 m. **h)** Feldspathic pyroxenite; BT-11-194/165.92 m. **i)** Melagabbro; BT-09-70/244.05 m. **j)** Mesogabbro; BT-12-234/211.33 m. **k)** Leucogabbro; BT-09-80/245.65 m. *l)* Anorthosite; BT-12-234/198.20 m. Younging direction in all photos is to the right. For the core shown in (d), (f), (i), (j), (k), and (l), the height (top to bottom) of the photo represents a core width of 4.7 cm; for all other photos, the height (top to bottom) of the photo represents a core width of 2.35 cm.

chromite-harzburgite, dunite, chromite, and olivine within a websterite matrix, forming a range of hybridized lithologies.

The Black Thor and Black Label chromitite horizons extend over a strike length of more than 3 km and 1.5 km, respectively. However, individual chromitite layers, particularly in Black Thor and the central parts of Black Label, are very difficult to follow along strike;

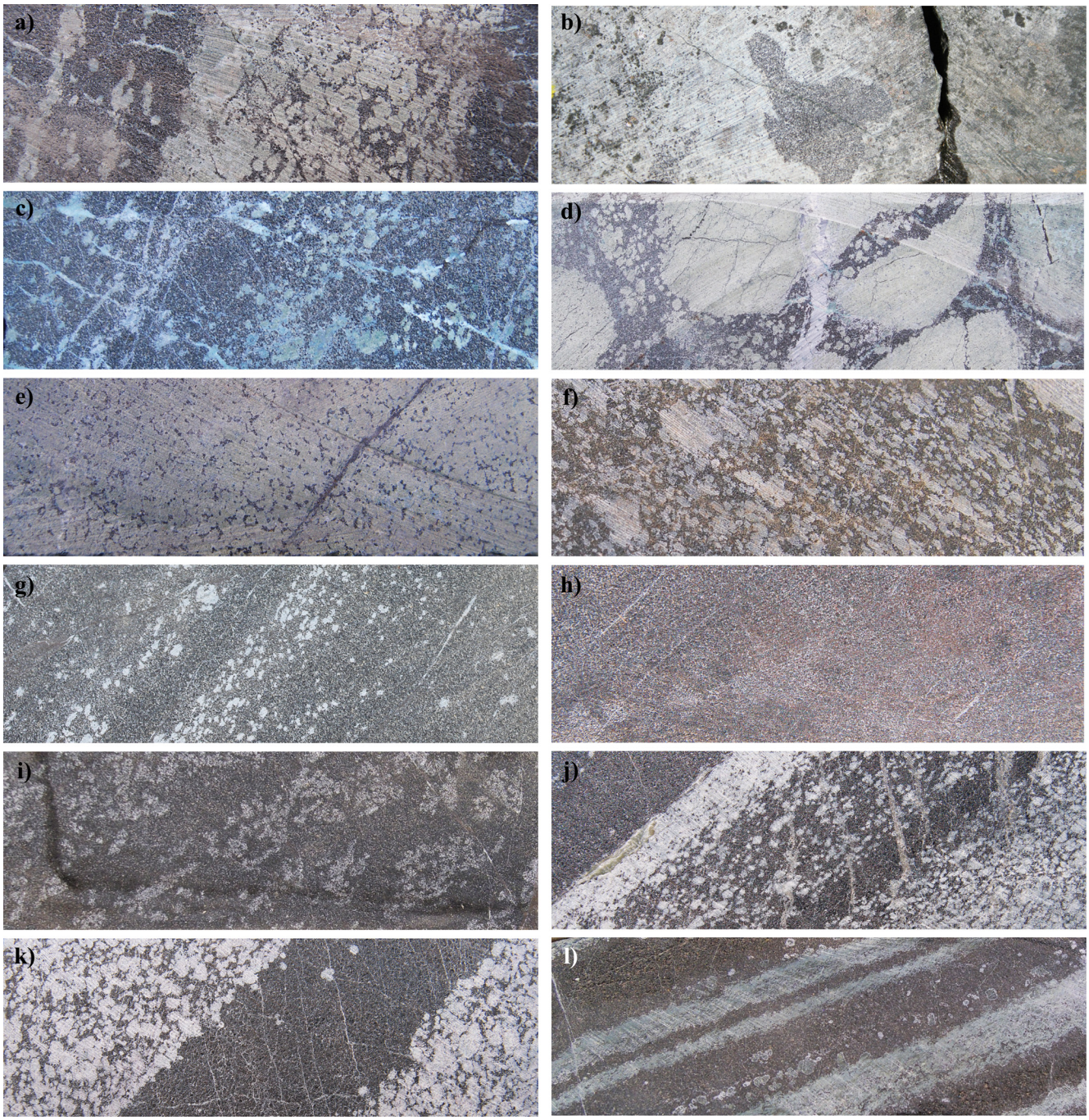

Figure 4. Photographs showing chromite textures of the Black Label chromitite horizon (a to d) and the Black Thor chromitite horizon (e to l) of the middle ultramafic series of the Black Thor intrusive complex. **a)** Massive chromitite layer with wavy, undulating upper contact against the matrix chromitite layer in serpentinized dunite, grading upwards into a massive chromitite layer; drill core BT-11-198/198.40 m. **b)** Blebby, co-mingling chromitite "clasts" hosted within late pyroxenite matrix; dril lcore BT-08-06/291.50 m. **c)** Semi-massive chromitite layer; drill core BT-11-198/195.07 m. **d)** Brecciated, matrix chromitite layer; drill core BT-11-198/199.00 m. **e)** Patchy net-textured chromitite, drill core BT-11-198/260.20 m. **f)** Matrix chromitite; drill core BT-11-196/548.74 m. **g)** Semi-massive chromitite; drill core BT-08-09/143.95 m. **h)** Massive chromitite; drill core BT-10-117/99.40 m. **i)** Mottled, semi-massive chromitite with "floating or suspended" serpentinized and/or pseudomorphed olivine grains; drill core BT-09-70/177.47 m. **j)** Massive chromitite layer with sharp upper contact against talc-tremolite-chlorite rock and serpentinized, pseudomorphed olivine, grading into semi-massive chromitite with a sharp upper contact against matrix chromitite layer; drill core BT-11-196/538.30 m. **k)** Matrix chromitite layer containing talc-tremolite-chlorite silicate minerals and serpentinized pseudomorphed olivine, with a sutured upper contact against a massive chromitite layer, in turn with a wavy, undulating upper contact against a matrix chromitite layer; drill core BT-11-196/559.30 m. **l)** Semi-massive chromitite layers alternating with continuous and semi-continuous serpentinized pseudomorphed olivine grain layers; drill core BT-10-113/172.17 m. Younging direction in all photographs is to the right. For the core shown in photographs (b), (d), (i), and (l), the height (top to bottom) of the photo represents a core width of 4.7 cm; for all other photographs, the height (top to bottom) of the photo represents a core width of 2.35 cm.

they are thicker and lenticular in the central part of the intrusion near and above the feeder zone and thinner and sheet-like away from the feeder zone. Pyroxene oikocrysts are more abundant in the central part of Black Thor horizon, where massive and semi-massive chromitite is common. Layers exhibiting normal modal grading (chromite-rich base and silicate-rich top) are more abundant in the lateral parts where matrix, net-textured, and disseminated chromitite is common. Layers containing intrafolial folds are only rarely observed.

Ni-Cu-(PGE) mineralization occurs dominantly in the lower ultramafic series of the BTIC. It includes multiple types and generations of mineralization (Farhangi et al., 2013): 1) early-magmatic mineralization along the basal contact of the intrusion; 2) intermediate-magmatic, sulphide-poor, PGE-rich, reef-style mineralization in the chromitite horizons; 3) intermediate-late-magmatic, sulphide-rich, PGE-poor, reef-style mineralization in fractionated gabbroic rocks of the mafic series; 4) late-magmatic, sulphide-rich mineralization associated with brecciation of the BTIC by the late websterite intrusion; and 5) tectonically/hydrothermally mobilized sulphide-rich mineralization within shear zones in the transition zone between the upper ultramafic and mafic series.

Whole-rock Geochemistry

The major element geochemical results reported here were obtained from drill core BT-11-196, which cuts through a part of the intrusion undisturbed by the LWI, and additional drill cores from the feeder zone (BT-09-67, BT-09-68, BT-09-69, BT-09-76, BT-10-115, BT-10-116, BT-10-117, BT-10-118, BT-10-119, BT-10-127, BT-10-135, BT-10-137, BT-10-138, BT-10-167, BT-1-182, BT-11-183, BT-11-184); these results are compared with the Cliffs XRF assay results of the entire deposit (Fig. 5). Three major trends are evident in MgO variation diagrams:

1. Mixing trends between olivine (~40% SiO_2, 45% MgO, and 8% FeO_t, with minor to negligible abundances of other elements — based on mineral analyzes and stoichiometry) and chromite (10–45% Cr_2O_3, 8% Al_2O_3, ~15% FeO_t, and 20–30% MgO, with minor to negligible abundances of other elements).
2. Mixing trends between olivine and orthopyroxene (~52% SiO_2, 3% Al_2O_3, ~10% FeO_t, ~30% MgO, and <5% CaO, with minor to negligible abundances of other elements).
3. Fractionation trends from the inferred parental magma (~46% SiO_2, ~9% Al_2O_3%, ~11% FeO_t, ~22% MgO, and ~8% CaO, with minor to negligible abundances of other elements — based on observed mineral assemblages and consistent with that proposed for Blackbird by Mungall et al., 2010) toward the leuco-, meso-, and melanogabbro in the upper part of the BTIC.

The majority of low-Cr samples on the loss-on-ignition (LOI) versus MgO diagram plot between hydrated websterite (30–35% MgO and 5–20% LOI) and serpentinized lherzolite/dunite ± chromitite (up to 25% LOI). The majority of high-Cr samples plot at lower MgO and/or higher LOI, reflecting higher degrees of carbonatization of the silicate components in chromitite. The cluster at low MgO and LOI represents least-altered mafic rocks of the upper series, whereas the cluster at 25–30% MgO and low LOI represents late websterite samples, which are the least altered rocks within the BTIC.

Low-Cr late websterite samples have low Ca and Al contents, indicating that they are composed primarily of orthopyroxene with only minor clinopyroxene or plagioclase (see Spath et al., 2015). High-Cr late websterite samples contain xenolithic and xenocrystic chromite incorporated from Black Label during emplacement.

The increase in Cr with decreasing Mg (Fig. 5) reflects accumulation of chromite with a chromite: olivine ratio well above the cotectic proportion of ~1:60 (e.g. Lesher and Stone, 1996; Barnes and Roeder, 2001); only a few samples lie on the cotectic (Fig. 6). This means that superimposed on the very small background abundance defined by the cotectic, chromite has been added through either (1) supersaturation (i.e. consistently precipitating extra chromite beyond the amount defined by the cotectic), (2) modifying the location of the cotectic (i.e. consistently precipitating more chromite with olivine than under normal conditions), or (3) mechanical accumulation of chromite in addition to that crystallized with olivine.

Chemostratigraphy

Lithogeochemistry has been plotted against depth and correlated with digitized stratigraphic logs to give an indication of the geochemical changes through the complex (Fig. 7). The overall trend within the ultramafic portion of the BTIC is one of decreasing Si-Fe-Mg and increasing Cr-Al-Ti-V. However, superimposed on this overall trend are (1) at the base of the complex, a reversal from Mg-poor olivine websterite to Mg-rich dunite that is interpreted to reflect more rapid cooling along the lower contact, which resulted in lower rates of accumulation of olivine at the base of the body; (2) many small reversals in the overall trend associated with chromite horizons and interlayering of dunite, lherzolite, and websterite; and (3) an abrupt decrease in Cr-Fe-Al-(Ti)-V and increase in Si-(Na-K) above the Black Thor chromite horizon, reflecting the upper mafic portion of the BTIC. Based on petro-

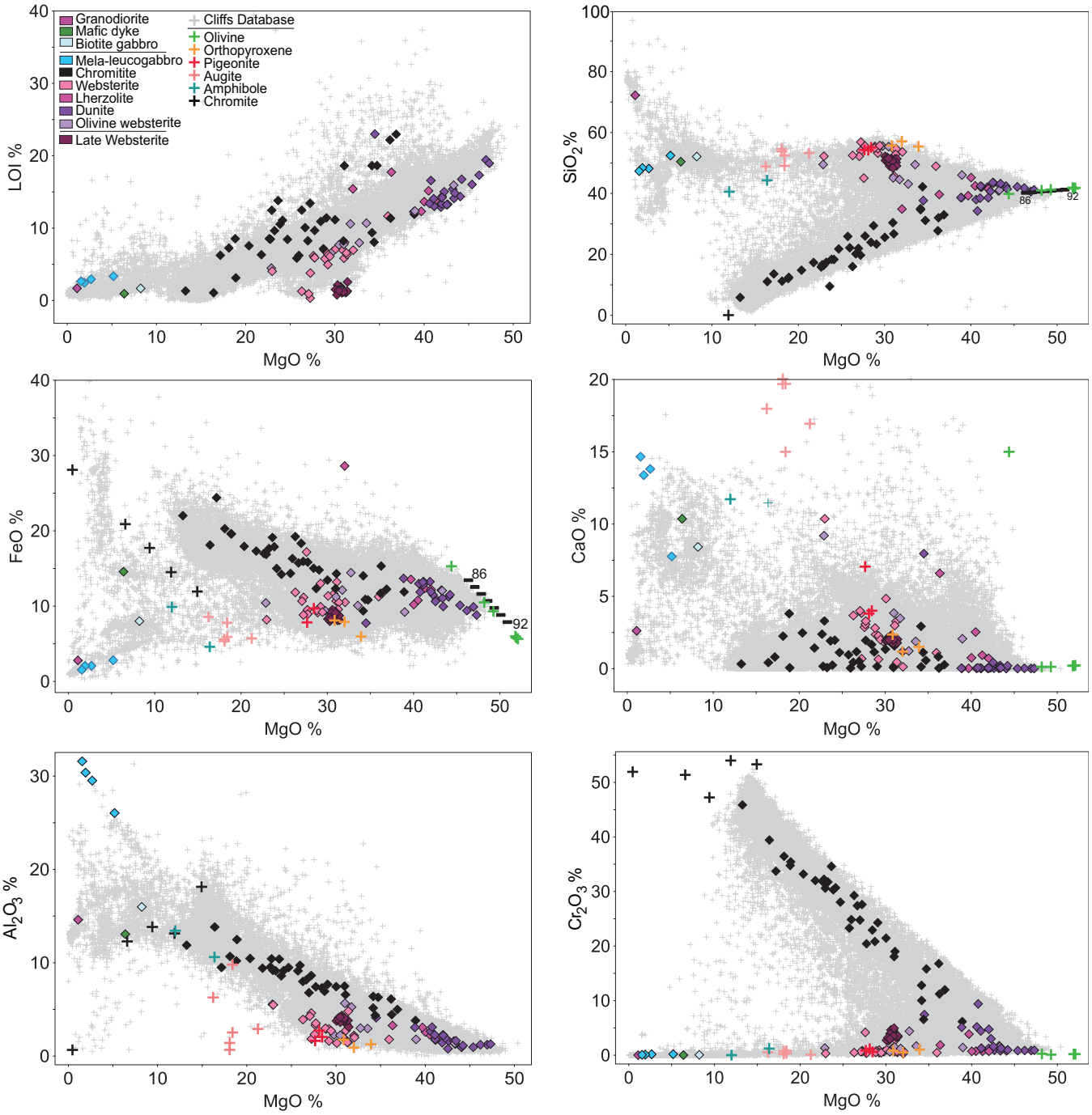

Figure 5. Major oxide versus MgO variation diagrams for samples from drillhole BT-11-196 (solid symbols). Also shown are compositions from a suite of samples from Cliffs Natural Resources database (pale grey crosses) and mineral compositions from Arndt et al. (2008; compiled from various sources, crossed symbols). In the MgO-SiO_2 and FeO-SiO_2 diagrams, 86 and 92 are mole percent forsterite contents in olivine, shown for reference. Abbreviations: FeO = total iron, LOI = loss on ignition.

graphic observations, this is interpreted to reflect a decreasing abundance of olivine and an increasing abundance of chromite with increasing stratigraphic height.

Trace Element Geochemistry

Most rock types exhibit negative Nb-Ta and variable Sr anomalies relative to Th, La, and LREEs, which is interpreted to represent addition of an upper continental crust component. U is enriched in some dunite and websterite samples, which is interpreted to reflect U mobility in metamorphic fluids. Positive Sr anomalies in chromite- and plagioclase-rich samples presumably reflect mobility of Sr and accumulation of plagioclase, respectively. Positive Ti anomalies in Cr-rich samples reflect enrichment in Ti in the minor ulvöspinel com-

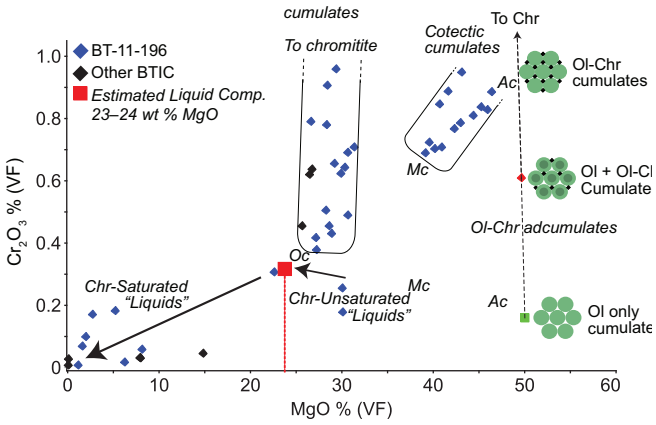

Figure 6. Mg-Cr diagram (note scale at 1% Cr_2O_3) highlighting samples that lie on the olivine:chromite cotectic (cotectic cumulates) and those that do not (non-cotectic cumulates), suggesting chromite has been added through supersaturation, modification of the cotectic, or mechanical accumulation (see text). Dashed line is the proportion of olivine:chromite from 100% olivine (green), 99:1 olivine:chromite (red square) along a mixing line to 100% chromite (not shown). No samples fall within the field for adcumulate at 100% olivine, indicating the liquid was already saturated in chromite during crystallization. Abbreviations: Ac = adcumulate, Chr = chromite; Mc = mesocumulate, Oc = orthocumulate textures; Ol = olivine.

ponent of chromite. Variable MREE/HREE ratios are interpreted to represent variable degrees of accumulation of olivine and orthopyroxene (Fig. 8).

Websterite (Fig. 8) also exhibits negative Nb-Ta anomalies relative to Th, La, and LREEs, but has negative Sr anomalies in Cr-poor samples and positive Sr and Ti anomalies in Cr-rich samples. Late websterite has systematically lower REE abundances and displays flatter MREE-HREE patterns, whereas BTIC websterite has systematically higher REE abundances, is more enriched in HILE-LREE relative to MILE, and displays steeper MREE-HREE patterns.

Gabbroic rocks exhibit the same negative Nb-Ta anomalies relative to Th, La, and LREEs, but exhibit large positive Sr and (for 2 of 3 samples) Eu anomalies, reflecting accumulation of plagioclase. The similarities of the trace element patterns of the mafic rocks with the ultramafic rocks provide further evidence to support the interpretation that they are co-magmatic.

Chromite Petrography and Chemistry

The BTIC chromite can be homogenous, or contain large (0.5–2 mm) spherical inclusions or abundant fine inclusions. Preliminary ED-XRES analyses of the coarse and fine inclusions indicate that they are composed of a serpentine-amphibole-chlorite-carbonate assemblage that, based on their similarity to the mineralogy of the interstitial liquid, likely represent melt inclusions that have been altered during serpentinization.

LA-ICP-MS maps (not shown) indicate that (1) homogenous chromite displays little or no chemical variation, however some grains show outward increases in Ti-V and decreases in Al-Cr, which is interpreted to represent re-equilibration with trapped silicate melt; (2) zoned chromite displays outer rims enriched in Mn-Fe-Co-Ni-Zn, which are interpreted to be associated with metamorphic overgrowth and mag-

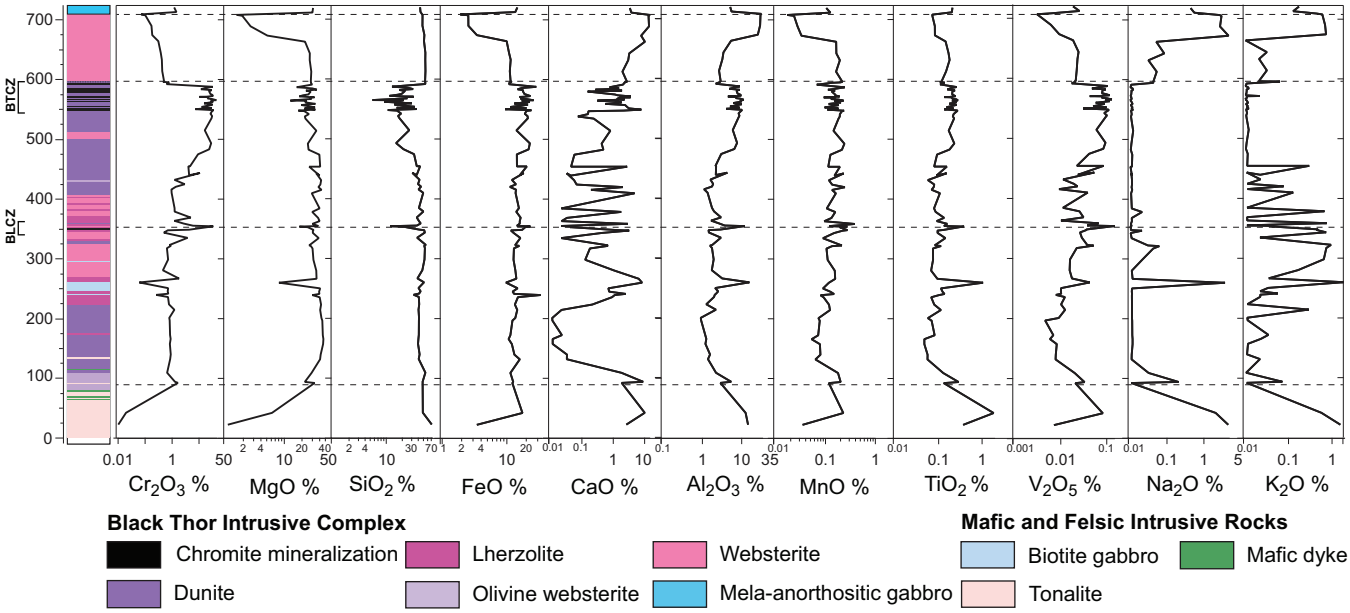

Figure 7. Whole-rock analytical results are plotted against depth in drillhole BT-11-196 and correlated with the stratigraphic log to illustrate the geochemical changes through the intrusive complex. The overall trend in the Black Thor intrusive complex (i.e. except for a basal reversal and small-scale variations) is one of decreasing Mg-Si with increasing Cr-Fe-Mn-Al-Ti-V. Abbreviations: BLCZ = Black Label (lower) chromitiferous zone; BTCZ = Black Thor (upper) chromitiferous zone.

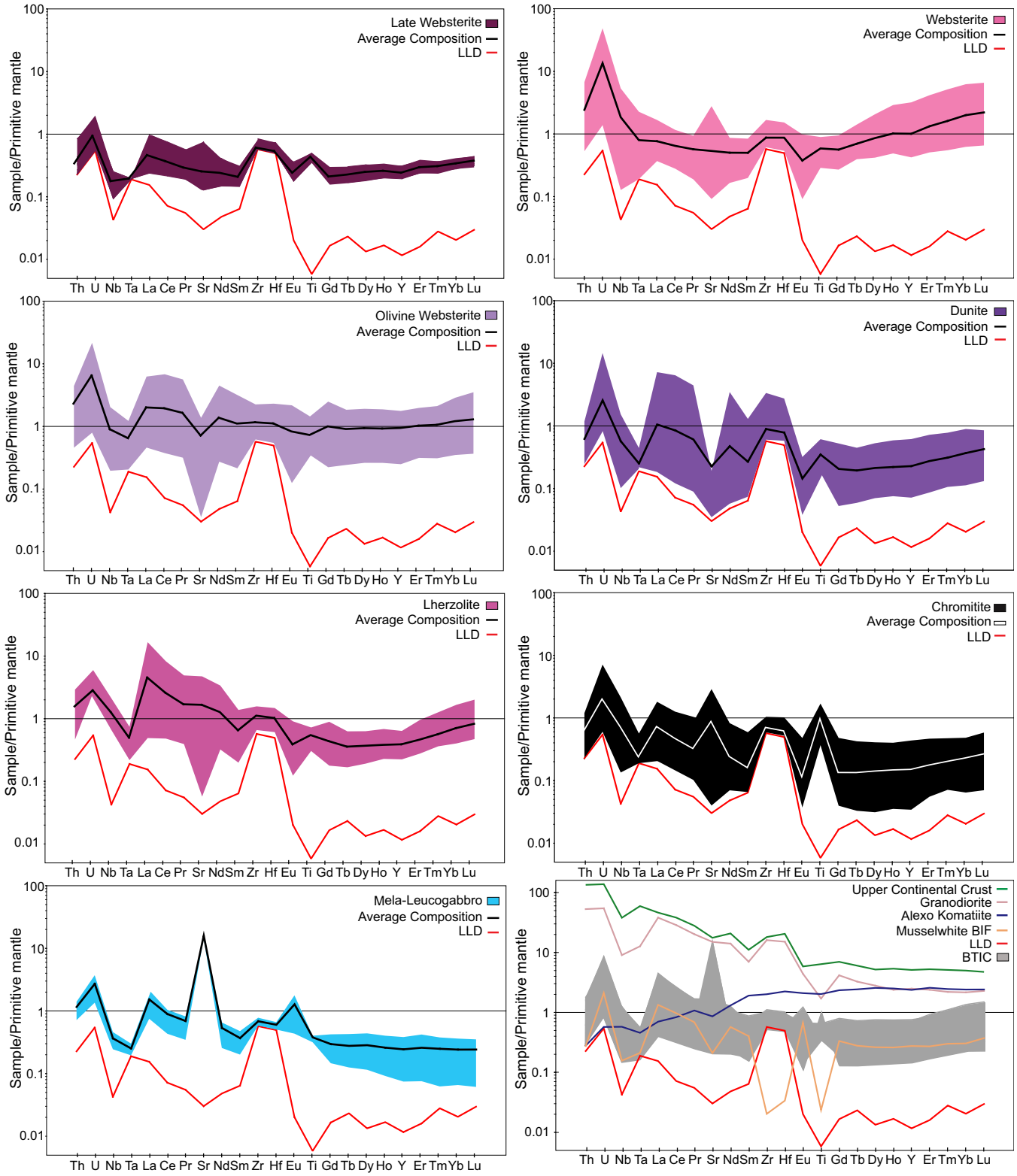

Figure 8. Rare earth element and trace element geochemistry from drillhole BT-11-196 and from reference data: Upper continental crust (Taylor and McLennan, 1985), Alexo komatiite (KAX-1 geochemical analysis by GeoLabs, Sudbury, ON), and Musselwhite banded iron formation (Gourcerol et al., 2013). Primitive mantle normalizing values are from McDonough and Sun (1995). Abbreviations: BIF = banded iron formation; BTIC = Black Thor intrusive complex; LLD = lower limit of detection.

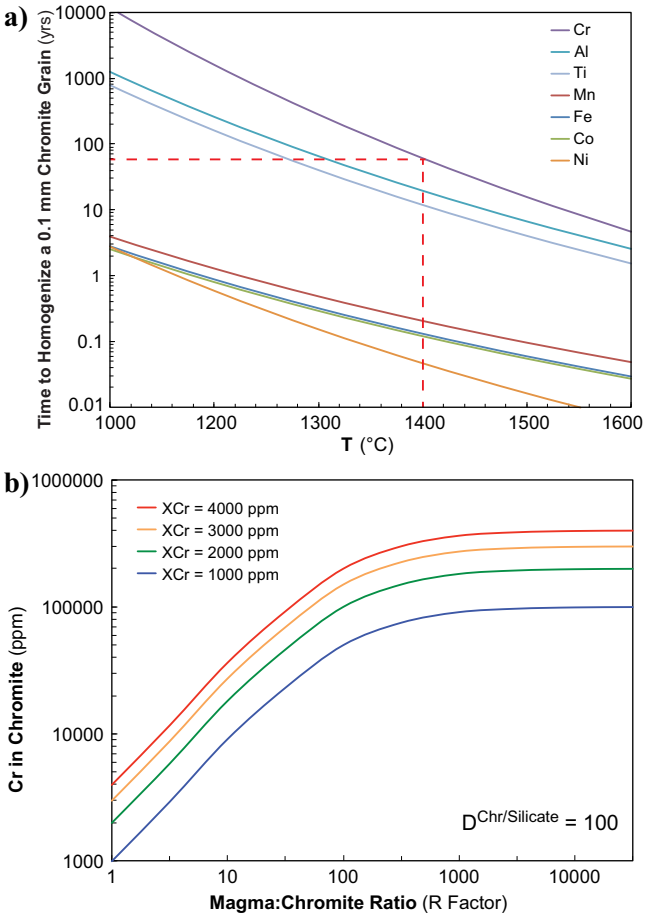

Figure 9. Magnetite diffusion and mass balance models. **a)** At 1400°C it would take approximately 50 years for Cr to diffuse through a 0.1 mm magnetite grain and transform it to chromite (diffusion constants from Dieckmann and Schmalzried, 1977; Dieckmann et al., 1978; Aggarwal and Dieckmann, 2002). **b)** Mass balance calculations estimate a komatiitic magma at ~3000 ppm Cr with chromite/magma partition coefficients of 100–200 for Cr, indicate a minimum magma:chromite ratio (R Factor) of 200 will upgrade magnetite to chromite.

netite alteration; and (3) inclusions in chromite layers are composed of serpentine ± chlorite ± amphibole ± calcite, which are interpreted to be serpentinized melt inclusions.

GENETIC MODEL

The fundamental problem in the understanding of the genesis of the BTIC is in inability to explain how such large quantities of chromite could accumulate from a magma that would normally crystallize chromite in only accessory abundances.

Most stratiform chromite deposits are hosted by large layered complexes that are interpreted to represent periodically replenished magma chambers (e.g. Bushveld Complex, South Africa; Stillwater Complex, USA). Genetic models for these deposits include (1) in situ crystallization associated with oxidation (Ulmer, 1969) or pressure increase (Lipin, 1993); (2) contamination and wholesale assimilation of felsic rocks or iron formation (Irvine, 1975; Rollinson, 1997); (3) magma mixing (e.g. Irvine, 1977; Campbell and Murck, 1993); and (4) physical transportation of fine-grained chromite in magmatic slurries (e.g. Eales, 2000; Mondal and Mathez, 2007; Maier et al., 2013). However, the Black Thor and Black Label chromitite deposits as well as several others (e.g. Kemi, Finland; Inyala and Railway Block, Zimbabwe; Ipueira-Medrado, Brazil; Sukinda, India; Nkomati, South Africa) are hosted by smaller intrusions that are interpreted to represents flow-through feeder sills and magma conduits that are stratiform in structure but lenticular in shape.

The much higher abundances of chromite in the latter deposits are not easily explained by the above processes, which has stimulated the development of a new model that involves partial melting of oxide-silicate-facies iron formation (OXIF) of the type observed in the footwall rocks (Fig. 1). Complete melting of OXIF is excluded due to the absence of Fe enrichment in the host rocks (Azar, 2010; Mungall et al., 2010). In the new model, silicate components (chert/quartz and Fe-silicate minerals) are melted and incorporated into the magma, accounting for the anomalous abundance of orthopyroxene in systems that should crystallize only very small amounts of orthopyroxene. However, magnetite cannot melt, because low-Mg komatiitic magmas, like the one in the BTIC, are saturated in chromite and therefore cannot incorporate any additional oxide. Very fine-grained disaggregated xenocrystic magnetite could be upgraded to chromite during transport, in the same way that barren sulphide xenomelts are interpreted to have been upgraded to form Ni-Cu-(PGE) deposits via interaction with komatiitic magma (see Lesher and Campbell, 1993).

Cr is one of the slower elements to diffuse in magnetite (Fig. 9a). Preliminary calculations indicate that at 1400°C (assuming komatiitic basalt magma composition) it would take approximately only 50 years to homogenize a 0.1 mm diameter magnetite grain and transform it into chromite. Considering that this is a dynamic flow-through system and that large mafic magmatic systems are typically active for 1–5 million years (e.g. continental flood basalt provinces and other large igneous provinces), this is more than enough time to completely re-equilibrate xenocrystic magnetite, especially if it started out as very fine grains. Mass balance calculations, using 2500–3500 ppm Cr in the magma and chromite/magma partition coefficients for Cr of 100–200, indicate that a magma:chromite ratio (R factor) as low as 200 is enough to transform magnetite into chromite (Fig. 9b). This range of R is well within the range estimated for many komatiite-associated Ni-

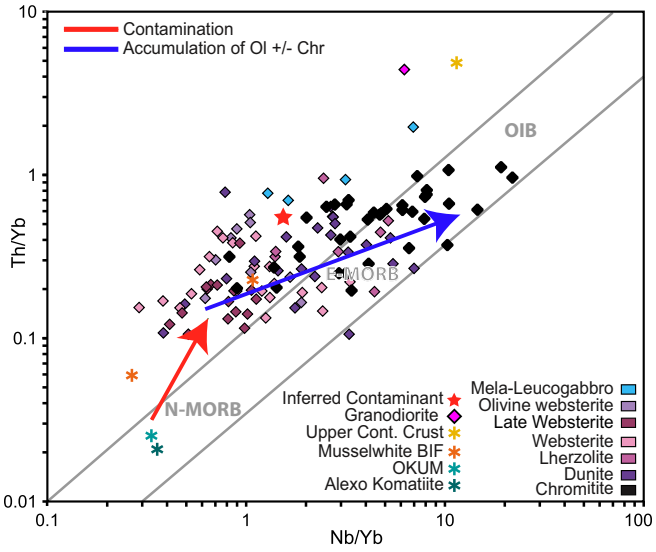

Figure 10. Nb-Th proxy diagram (designed for oceanic basalts but valid for olivine-pyroxene cumulates, assuming that Th-Nb-Yb are housed in the interstitial liquids rather than the cumulus minerals) highlighting the contamination evolution of Black Thor intrusion complex rocks, from an N-MORB source (KAX-1 Alexo komatiite and OKUM komatiite reference material from the GeoLabs, Sudbury, Ontario) towards an inferred contaminant (star, indicated by red line) based on mixing average upper continental crust (Taylor and McLennan, 1985) and granodiorite from the Black Thor intrusive complex (1330501, drill core BT-11-196/22.50 m) with oxide-facies iron formation (Musselwhite banded iron formation (BIF); Gourcerol et al., 2015), resulting in a higher Th/Yb ratio. Accumulation of olivine and chromite is highlighted by a large spread in the Nb/Yb ratio (indicated by the blue line). Abbreviations: Chr = chromite; Ol = olivine.

Cu-(PGE) systems (e.g. Kambalda, Perseverance, Raglan: Lesher and Keays, 2002).

The trace element geochemical data exhibit considerable scatter because of the very low abundances (near the detection limits) of such elements in olivine ± chromite ± pyroxene cumulates, but they suggest contamination by rocks of the upper continental crust. Iron formations contain low abundances of trace elements (Figs. 7. 9), indicating that although considerable amounts of iron formation could be present as a contaminant, it cannot be the source of the pronounced HILE enrichment relative to MILE and HREE. Rocks of the upper continental crust, such as the footwall tonalite-granodiorite, are sufficiently enriched in HILE (relative to MILE-HREE) to be the source of the pronounced enrichment in BTIC rocks, but they are too enriched in Th relative to Yb and too enriched in Nb relative to Yb to produce the geochemical signatures of the olivine – chromite-poor samples. So, a combination of contaminants is required. The presence of these signatures in all of the rocks suggests contamination at depth, not in the BTIC itself.

Partial assimilation of OXIF and the upgrading of magnetite to chromite, in conjunction with contamination by rocks of the upper continental crust, could be key to the formation of the BTIC mineralization (and other conduit-hosted stratiform deposits). In order for this mechanism to be feasible (Fig. 10), the following are required: (1) a Cr-rich komatiitic magma, (2) the presence of sufficient oxide-facies iron formation near or below the stratigraphic level of the intrusion, and (3) a flow-through magmatic system with sufficient flux to transport fine magnetite grains and allow them to interact with the Cr-rich magma. Additional work is planned to further evaluate this process.

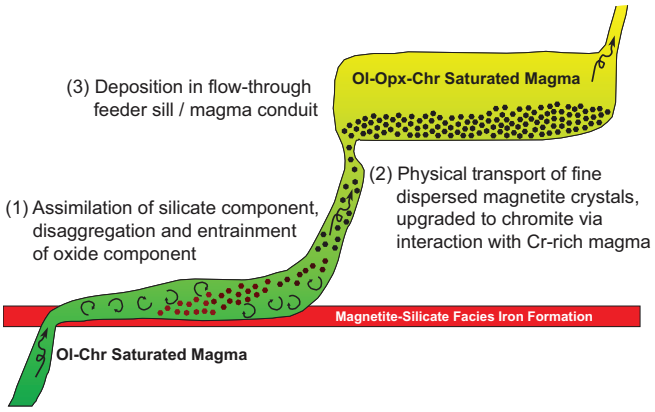

Figure 11. Preliminary schematic model of the partial-assimilation and magnetite-upgrading process proposed in this study. (1) Magma saturated in olivine and chromite is intruded into magnetite-bearing oxide-silicate-facies iron formation, partially assimilating it by dissolving the silicate component (chert, quartz, and Fe-silicate minerals) but not the oxide component; (2) fine-grained magnetite grains are disaggregated and transported within the magma conduit, where they interact with the Cr-rich magma and, via diffusion, are enriched in Cr and upgraded to chromite; (3) lastly, the chromite is deposited in the feeder sill / magma conduit. Abbreviations: Chr = chromite; Ol = olivine; Opx = orthopyroxene.

IMPLICATIONS FOR EXPLORATION

The new genetic model proposed in this study has many important implications that could help target mineral exploration for this type of chromite deposit.

- Exploration should focus on areas where high-Cr, low-Mg komatiitic magma is present. Higher Mg komatiitic magma may be less prospective, as they are not saturated in chromite. Some prospective magma is Archean but many are early Proterozoic.
- Exploration should focus on areas where oxide-facies (rather than sulphide-facies) iron formation is present.
- Exploration should focus on areas where olivine ± orthopyroxene cumulates are present (rather than olivine-only cumulates).

This study highlights the proposition that small, Archean, ultramafic-dominated intrusions like the

BTIC can not only host large chromite deposits but also contain significant Ni-Cu-(PGE) mineralization.

ACKNOWLEDGEMENTS

We would like to thank R. Metsaranta and B. Azar (Ontario Geological Survey), and R. Weston, D. Shinkle, and Bryan Maciag (Cliffs Natural Resources Inc.) for their help and insightful discussions. We are very grateful to R. Fink and A. Mitchell (Cliffs Natural Resources Inc.) for logistical support and access to the property and geological databases, and to the team in Esker Camp for their assistance during the 2012 and 2013 field seasons. Financial support is being provided by the NSERC-CRD, NSERC Discovery, and Geological Survey of Canada TGI-4 programs, the Ontario Geological Survey, and the Society of Economic Geologists Student Research Grant program. Joe Petrus (LU), Dave Crabtree, and Sandra Clarke (GeoLabs) provided assistance in LA-ICP-MS analysis and EMPA/SEM/XRD analysis, respectively. We are also grateful to T. Clark (MERNQ) for many helpful editorial suggestions that significantly improved this contribution.

REFERENCES

Aggarwal, S. and Dieckmann, R., 2002. Point defects and cation tracer diffusion in $(Ti_xFe_{1-x})_{3-\delta}O_4$. II. Cation tracer diffusion; Physics and Chemistry of Minerals, v. 29, p. 707–718.

Arndt, N., Lesher, C.M., and Barnes, S.J., 2008. Komatiite, 1st edition; Cambridge University Press, Cambridge, United Kingdom, 467 p.

Azar, B., 2010. The Blackbird chromite deposit, James Bay Lowlands of Ontario, Canada: Implications for chromitite genesis in ultramafic conduits and open magmatic systems; M.Sc. thesis, University of Toronto, Toronto, Ontario, 154 p.

Barnes, S.J. and Roeder, P.L., 2001. The range of spinel compositions in terrestrial mafic and ultramafic rocks; Journal of Petrology, v. 42, p. 2279–2302.

Campbell, I.H. and Murck, B.W., 1993. Petrology of the G and H chromitite zones in the Mountain View area of the Stillwater complex, Montana; Journal of Petrology, v. 34, p. 291–316.

Carson, H.J.E., Lesher, C.M., Houlé, M.G., Weston, R.J., Metsaranta, R.T., and Shinkle, D.A. 2013. Komatiite-associated Cr and Ni-Cu-(PGE) mineralization in the Black Thor–Black Label ultramafic intrusive complex, McFaulds Lake greenstone belt, *In:* Proceedings; 12th Biennial SGA Meeting, Uppsala, Sweden, August 12-15, 2013, p. 960–963.

Dieckmann, R. and Schmalzried, H., 1977. Defects and cation diffusion in magnetite; Reports of the Bunsen Society for Physical Chemistry, v. 81, p. 344–347.

Dieckmann, R., Mason., T.O., Hodge, J.D., and Schmalzried, H., 1978. Defects and cation diffusion in magnetite (III.) Tracer diffusion of foreign tracer cations as a function of temperature and oxygen potential; Reports of the Bunsen Society for Physical Chemistry, v. 82, p. 778–783.

Eales, H.V., 2000. Implications of the Cr budget of the western limb of the Bushveld Complex; South Africa Journal Geology, v. 103, p. 141–150

Farhangi, N., Lesher, C.M., and Houlé, M.G., 2013. Mineralogy, Geochemistry and Petrogenesis of Nickel-Copper-Platinum Group Element Mineralization in the Black Thor Intrusive Complex, McFaulds Lake Greenstone Belt, Ontario, *In:* Summary of Field Work and Other Activities 2013; Ontario Geological Survey, Open File Report 6290, p. 55-1 to 55-7.

Gourcerol, B., Thurston, P.C., Kontak, D.J., Côté-Mantha, O., and Biczok, J., 2015. Distinguishing primary and mineralization-related signatures of chert from the banded iron-formation-hosted gold deposits at Musselwhite, Ontario and Meadowbank, Nunavut; Geological Survey of Canada, Current Research 2015-1, 21 p.

Irvine, T.N., 1975. Crystallization sequences in the Muskox Intrusion and other layered intrusions II. Origin of chromite layers and similar deposits of other magmatic ores; Geochimica et Cosmochimica Acta, v. 39, p. 991–1020.

Irvine, T.N., 1977. Origin of the chromite layers in the Muskox Intrusion and other stratiform intrusions: A new interpretation; Geology, v. 5, p. 273–277.

Laarman, J.E., 2014. A detailed metallogenic study of the McFaulds Lake chromite deposits, northern Ontario; Ph.D. thesis, University of Western Ontario, London, Ontario, 529 p.

Lesher, C.M. and Campbell, I.H., 1993. Geochemical and fluid dynamic modeling of compositional variations in Archean komatiite-hosted nickel sulfide ores in Western Australia; Economic Geology, v. 88, p. 804–816.

Lesher, C.M. and Keays, R.R., 2002. Komatiite-associated Ni-Cu-(PGE) deposits: mineralogy, geochemistry, and genesis, *In:* The Geology, Geochemistry, Mineralogy, and Mineral Beneficiation of the Platinum-Group Elements, (ed.) L.J. Cabri; Canadian Institute of Mining, Metallurgy and Petroleum, Special Volume 54, p. 579–617.

Lesher, C.M. and Stone, W.E., 1996. Exploration geochemistry of komatiites, *In:* Igneous Trace Element Geochemistry: Applications for Massive Sulphide Exploration; Geological Association of Canada, Short Course, v. 12, p. 153–204.

Lipin, B.R., 1993. Pressure increases, the formation of chromite seams, and the development of the Ultramafic Series in the Stillwater Complex, Montana; Journal of Petrology, v. 34, p. 955–976.

Maier, W.D., Barnes, S.-J., and Groves, D.I., 2013. Bushveld formation of Pt-Pd, Cr, V-rich layers via hydrodynamic sorting of mobilised cumulate slurry in a large, relatively slowly cooling, subsiding magma chamber; Mineralium Deposita, v. 48, p. 1–56.

McDonough, W.F. and Sun, S.-S., 1995. Composition of the Earth; Chemical Geology, v. 120, p. 223–253. doi:10.1016/0009-2541(94)00140-4

Mehrmanesh, K., Carson, H.J.E., Lesher, C.M., and Houlé, M.G., 2013. Stratigraphy, geochemistry and petrogenesis of the Black Label chromitite horizon, Black Thor Intrusive Complex, McFaulds Lake Greenstone Belt, Ontario, *In:* Summary of Field Work and Other Activities 2013; Ontario Geological Survey, Open File Report 6290, p. 53-1 to 53-6.

Mondal, S.K. and Mathez, E.A., 2007. Origin of the UG2 chromitite layer, Bushveld Complex; Journal of Petrology, v. 48, p. 495–510.

Mungall, J.E., Harvey, J.D., Balch, S.J., Azar, B., Atkinson, J., and Hamilton, M.A., 2010. Eagle's Nest: A magmatic Ni-sulfide deposit in the James Bay Lowlands, Ontario, Canada, *In:* The Challenge of Finding New Mineral Resources: Global Metallogeny, Innovative Exploration, and New Discoveries, Volume I: Gold, Silver, and Copper-Molybdenum, (ed.) R.J. Goldfarb, E.E. Marsh, and T. Monecke; Society of Economic Geologists, Special Publication 15, p. 539–559.

Mungall, J.E., Azar, B., and Hamilton, M., 2011. Ni-Cu-PGE-Cr-Fe-Ti-V and VMS mineralization of the Ring of Fire intrusive suite, Ontario, *In:* Program with Abstracts; Geological Association of Canada-Mineralogical Association of Canada-Society of Economic Geologists-Society for Geology Applied

to Mineral Deposits (GAC-MAC-SEG-SGA) joint meeting, Ottawa, May 25-27, 2011, v. 34, p. 148.

Rollinson, H., 1997. The Archean komatiite-related Inyala chromitite, southern Zimbabwe; Economic Geology, v. 92, p. 98–107.

Spath, C.S. III, Lesher, C.M., and Houlé, M.G., 2015. Hybridized ultramafic rocks in the Black Label hybrid zone of the Black Thor intrusive complex, McFaulds Lake greenstone belt, Ontario, *In:* Targeted Geoscience Initiative 4: Canadian Nickel-Copper-Platinum Group Elements-Chromium Ore Systems — Fertility, Pathfinders, New and Revised Models, (ed.) D.E. Ames and M.G. Houlé; Geological Survey of Canada, Open File 7856, p. 103–114.

Taylor, S.R. and McLennan, S.M., 1985. The Continental Crust: It's Composition and Evolution, An Examination of the Geochemical Record Preserved in Sedimentary Rocks; Blackwell Scientific Publication Inc., Palo Alto, California, 328 p.

Tuchscherer, M.G., Hoy, D., Johnson, M., Shinkle, D., and Holmes, M., 2010. Fall 2008 to winter 2009 technical drill report on the Black Thor chromite deposit-Black Label chromite zone and associated Ni-Cu-PGEs, McFaulds Lake property, James Bay Lowlands, Northern Ontario; Internal technical report, Freewest Resources Canada Inc., filed February 2010, 57 p.

Ulmer, G.C., 1969. Experimental investigations of chromite spinels, *In:* Magmatic Ore Deposits, (ed.) H.D.B. Wilson; Society of Economic Geologists, Monograph 4, p. 114–131.

Weston, R. and Shinkle, D.A., 2013. Geology and stratigraphy of the Black Thor and Black Label chromite deposits, James Bay Lowlands, Ontario, Canada, *In:* Proceedings; 12th Biennial SGA Meeting, Uppsala, Sweden, August 12–15, 2013, p. 1069–1071.